Soft Matter

PAPER

View Article Online
View Journal | View Issue

Cite this: *Soft Matter*, 2015, **11**, 3222

Critical adsorption of a flexible polymer on a stripe-patterned surface

Hong Li,*[ab] Bin Gong,[b] Chang-Ji Qian[a] and Meng-Bo Luo[c]

Received 19th February 2015
Accepted 2nd March 2015

DOI: 10.1039/c5sm00426h

www.rsc.org/softmatter

The adsorption and dynamics of a polymer chain on a stripe-patterned surface composed of periodical attractive and neutral stripes are studied by using Monte Carlo simulation. The critical adsorption temperature T_c and pattern-recognition temperature T_r are estimated from the desorption probability, surface contact number, and bridge number. A phase diagram presenting three polymer states, including a desorbed state above T_c, a multi-stripe adsorbed state at an intermediate temperature $T_r < T < T_c$, and a single-stripe adsorbed state below T_r, is provided for infinitely long chains. Normal diffusion is always observed for a polymer in the direction parallel to the stripe even at low temperature. But in the direction perpendicular to the stripe, the polymer can freely diffuse above T_c, whereas the polymer is confined to one attractive stripe below T_r. However, the adsorbed polymer can hop from one attractive stripe to another at the intermediate temperature $T_r < T < T_c$.

1. Introduction

The properties of adsorption and diffusion of polymers near surfaces have received extensive attention from both theory and experiment.[1–4] Properties of a polymer adsorbed on surfaces are important in various areas of science and technology such as adhesion, lubrication,[5] chromatography,[6] gel permeation, stabilization,[7] DNA segregation,[8] and DNA packaging in viruses.[9]

The details of the adsorption transition of a homogeneous polymer on a homogeneous surface have been well studied.[10–16] Whether a polymer chain is adsorbed on or desorbed from an attractive surface is dependent on the strength of the polymer–surface attraction. At the critical adsorption point (CAP), a transition from a desorbed state at weak polymer–surface attraction to an adsorbed state at strong attraction occurs.[10–16] The conformational properties of polymers, such as the conformational size and shape, are also dependent on the strength of the polymer–surface attraction.[15] The structure of adsorbed polymer chains is usually characterized by the terms trains, loops and tails. A train consists of continuously adsorbed monomers, a loop is a connection between trains, and a tail is a desorbed part at the end of a chain.[17] The number of monomers involved in a train, tail and loop is dependent on the polymer–surface attraction or temperature.[18] On the other hand, the polymer can diffuse along the surface even if it is adsorbed on the surface.[13]

The conformational properties and dynamics of a polymer on a heterogeneous surface are interesting but more complicated. A simple case of a heterogeneous surface is a stripe-patterned surface which is composed of two types of stripes distributed periodically on the surface.[19] And the two types of stripes have different polymer–surface interactions. Such a stripe-patterned surface and other ordered patterned surfaces were created in experiments by covering the surface with periodically distributed polar and non-polar chemical compounds[20–22] or by excavating holes on the substrate.[23] The self-organization of polymers on the periodic stripe-patterned surface has been a topic of recent research.[24–27] The strength of the polymer–surface interaction and the stripe width are two important controlling factors for the adsorption of polymers. It was found that an ordered film could be modulated by turning the polymer–surface attractive energy or by adjusting the stripe width.[28] The adsorption of polymers was also dependent on the polymer stiffness. It was found that the surface coverage of adsorbed polymers increased upon increasing the stiffness.[29] Polymer recognition is another important issue for the adsorption of polymers on patterned surfaces.[19,30–32] The pattern recognition process was analyzed as a function of the stripe width, the chain length, *etc.*[19] The polymer was confined in one stripe below the pattern-recognition temperature T_r. It was found that T_r is dependent on the polymer length, polymer stiffness, and stripe width. T_r is expected to be lower than the characteristic adsorbing temperature.[19]

The adsorption of polymer chains on the patterned surface is strongly influenced by surface properties due to the different polymer–surface interactions for polymers in contact with different stripes. But there are many mechanisms that are still

[a]*Department of Physics, Wenzhou University, Wenzhou 325035, China. E-mail: LiHong@wzu.edu.cn*

[b]*School of Computer Science and Technology, Shandong University, Jinan 250100, China*

[c]*Department of Physics, Zhejiang University, Hangzhou 310027, China*

unknown even for the adsorption and dynamical properties of a single polymer chain on patterned surfaces.[33] The influence of the stripe-patterned surface on the structure of an adsorbed polymer is interesting from the theoretical and experimental investigations. However, it is still difficult to determine the size and the shape of the single polymer chain adsorbed on the stripes by experiments. Therefore, computer simulations play important roles in understanding the underlying physics for the adsorption of polymers on patterned surfaces.[31,34–38] The adsorption of a negatively charged polyelectrolyte onto a positive–neutral stripe-patterned surface has been investigated by using Monte Carlo (MC) simulations. The adsorption fraction increased with the increase in the stripe width because large positive regions accommodated the negatively charged polymers more easily.[39] The attractive–repulsive striped pattern appeared as a neutral surface to the polymer when the stripe width was small compared to the polymer size. However, the polymer was confined within a single attractive stripe when the stripe width was wide enough.[39]

Although there is significant progress in understanding the adsorption of polymers on patterned surfaces, it is still incomplete and only a few studies reported the adsorption of a single polymer on a stripe-patterned surface. For a polymer adsorbed simultaneously on two attractive stripes, the competition between the attraction effect and the repulsion effect of the stripes would make the problem more complicated. In this work we present and discuss the results of MC simulations concerning a flexible polymer chain above a stripe-patterned surface with alternate attractive and neutral stripes. Our main goal is to study the critical adsorption of the homogeneous polymer on the stripe-patterned surface and the equilibrium and dynamic properties of the adsorbed polymer. We define the critical adsorption temperature T_c and the pattern-recognition temperature T_r of the polymer from the polymer equilibrium states. We find that both T_c and T_r have a similar scaling relationship with the stripe width. Then we provide a phase diagram presenting three equilibrium states of the polymer: a desorbed state above T_c, multi-stripe adsorbed state at intermediate temperature $T_r < T < T_c$, and single-stripe adsorbed state below T_r. The properties of the adsorbed polymer are strongly dependent on the equilibrium phase. In the multi-stripe adsorbed state at $T_r < T < T_c$, the adsorbed polymer adopts structures containing trains, loops, bridges (loops crossing two attractive stripes), and tails, and the adsorbed polymer may detach from one stripe and hop to the neighboring stripe after a certain period of time. Whereas in the single-stripe adsorbed state at $T < T_r$, the adsorbed polymer is fully adsorbed (train structure) on one attractive stripe, and the neighborhood hop is not observed.

2. Simulation model and calculation method

The simulation system is embedded in a simple cubic lattice. The lattice unit is set as the length unit in this paper. The stripe-patterned surface, composed of alternately distributed attractive–neutral stripes along the x axis as shown in Fig. 1, is placed at $z = 0$ parallel to the xy plane. The attractive stripes are marked as stripe A, while the neutral stripes are marked as stripe B. A polymer is placed above the surface. The nearest neighbor (NN) interactions between the polymer and the surface are taken into account. Specifically, we denote $-\varepsilon_A$ and $-\varepsilon_B$ as the energies between the polymer and the stripes A and B, respectively, for the polymer monomer located at the NN site of the surface, *i.e.* on the layer $z = 1$. The polymer monomer located at the NN site of the surface is named as a contact. The total energy of the system is

$$E = -\varepsilon_A n_A - \varepsilon_B n_B, \quad (1)$$

where n_A and n_B are the contact numbers of polymers with stripes A and B, respectively. Here we consider a simple case where each stripe is of identical width L along the x axis. Whereas the length along the y axis is infinite, it is achieved by a periodic boundary condition (PBC) along the y axis. PBC is also adopted for the system along the x axis to mimic a large surface. In this work, we set ε_A as the unit of energy and ε_A/k_B as the unit of temperature, where k_B is the Boltzmann constant. For simplification, we set $\varepsilon_A = 1$ as the stripe A is attractive to the polymer and $\varepsilon_B = 0$ as the stripe B is neutral to the polymer. In this work, the temperature T is a variable.

The homogeneous self-avoiding walk (SAW) polymer is composed of N sequentially linked identical monomers. Each monomer can be treated as a unit representing several atoms of a real polymer. Each monomer occupies one lattice site. Every lattice site cannot be occupied simultaneously by two or more monomers owing to the effect of the excluded volume of monomers. In our work, the improved bond fluctuation model (BFM) for a SAW polymer chain is adopted.[13,16,40] The bond length can be fluctuated as 1, $\sqrt{2}$ or $\sqrt{3}$ lattice units.[13,16,40] The simulation is carried out for a single polymer chain, *i.e.* for the case of an infinitely dilute polymer solution. A sketch of a polymer chain on the stripe-patterned surface is shown in Fig. 1. Here we refer to the bridge as the special loop that

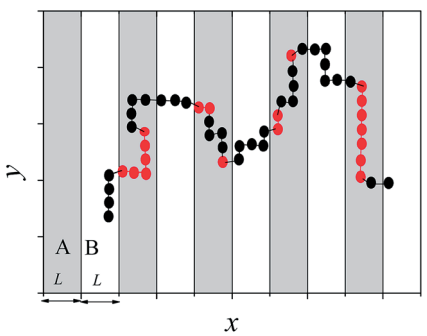

Fig. 1 Sketch of a polymer adsorbed on the stripe-patterned surface. The gray stripe denotes the attractive surface A and the light one denotes the inert surface B. Red circles represent adsorbed monomers, while the black ones represent desorbed monomers. Looking from the left: a tail (4 monomers), a train (6 monomers), a bridge (7 monomers), a train (2 monomers), and a loop (4 monomers).

connects trains on two different attractive stripes. In our simulations the system sizes in both x and y directions are larger than the polymer length, thus the polymer chain will not interact with its mirror images.

To confine the polymer to the system, an additional neutral homogeneous surface located at $z = D$ is introduced. This neutral surface can prevent the polymer from diffusing far away from the patterned surface. It is in this sense that we believe that this top neutral surface can mimic the solution–air interface in experiments. In the simulation, we use a large separation $D > N^{\nu}b_l$ to reduce the size effect due to the additional neutral surface.[13] Here $b_l \approx 1.42$ is the mean bond length of the polymer and $\nu \approx 0.588$ for a 3D SAW chain. The interaction between the polymer and the additional neutral surface is simply set as $\varepsilon = 0$. For example, we use the surface separation $D = 60$ for $N = 200$ ($N^{\nu}b_l \approx 30$).

At the beginning of the simulation, a SAW polymer chain is generated using the Rosenbluth–Rosenbluth chain generation method confined between the two surfaces.[38] It then undergoes Brownian motion for a long time to reach an equilibrium state. In the dynamic MC simulation, a trial move is achieved by randomly picking a monomer and attempting to move it randomly to one of the six NN sites.[13] If this trial move does not break the chain connectivity condition and avoid the excluded volume, we use the Metropolis algorithm to determine the trial move by accepting it with a probability equal to the minimum of 1 and the Boltzmann factor $\exp(-\Delta E/k_BT)$, *i.e.*

$$P_{\text{old}\to\text{new}} = \min[1, \exp(-\Delta E/k_BT)]. \quad (2)$$

Here $P_{\text{old}\to\text{new}}$ is the acceptant probability of the transition from the old configuration to the new one, where ΔE is the energy shift due to the trial move and T is the temperature. In one MC step (MCS) all monomers in the chain are attempted to move once on average. MCS is used as the unit of time in the simulations.

3. Results and discussion

3.1. Relaxation time

We investigate the dependence of the configuration properties of a polymer at different temperatures by annealing the system from a high temperature $T = 6.0$ to a low temperature $T = 0.05$. Using the annealing method, the last equilibrium conformation at the previous temperature is used as the starting conformation for the next temperature.[41–45] The temperature annealing procedure was also used previously in atomistic simulations.[46,47] Compared to single temperature simulation, the annealing method can significantly reduce the equilibrium time and therefore save simulation time.[41,44] In our simulation, we slowly decrease the temperature with a variable temperature step for $T > 2.0$ and a small step $\Delta T = 0.05$ for $T < 2.0$. We have checked the equilibrium of the system for the annealing method. To this end, the evolutions of $\langle R_G{}^2\rangle$ at $T = 0.2$, 0.7, and 2.0 are plotted in Fig. 2a for $N = 100$ and $L = 5$ as an example. We find that $\langle R_G{}^2\rangle$ reaches its equilibrium value quickly. The time for reaching equilibrium is smaller than the preset equilibrium time 50 000 ($\sim 2.5N^{2.13}$) for $N = 100$ used in the simulation. For comparison, the evolutions of $\langle R_G{}^2\rangle$ from the quenching method, where the simulation temperature of the system is arbitrarily set, are provided. At $T = 2.0$, two curves almost overlap except at the very beginning. At $T = 0.7$, two curves overlap at time 300 000 MCS, which is much longer than 50 000 MCS in the annealing method. However, at $T = 0.2$, it is extremely difficult to arrive at an equilibrium for the quenching method. It is clear that the annealing method can save the simulation time. For this reason, we adopt the annealing method in this paper.

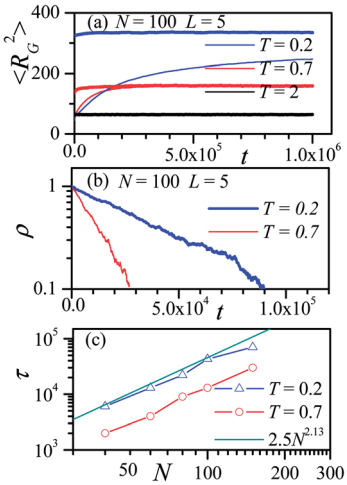

Fig. 2 (a) Evolution of $\langle R_G{}^2\rangle$ at $T = 0.2$, 0.7, and 2.0, thick lines are for the annealing method, while thin lines are for the quenching method. (b) The relaxation function $\rho(t)$ for $T = 0.7$ and 0.2. (c) Dependence of the longest relaxation time τ on N for $T = 0.7$ and 0.2.

The equilibration dynamics can be quantified by defining a relaxation function $\rho(t)$ for the square radius of gyration:

$$\rho(t) = \frac{\langle R_G{}^2\rangle_t - \langle R_G{}^2\rangle_{\text{eq}}}{\langle R_G{}^2\rangle_0 - \langle R_G{}^2\rangle_{\text{eq}}} \quad (3)$$

where $\langle R_G{}^2\rangle_t$ and $\langle R_G{}^2\rangle_0$ are the mean square radius of gyration at time t and at time $t = 0$, respectively. Here $\langle\ \rangle$ is averaged over the samples. Fig. 2b shows the evolution of $\rho(t)$ at $T = 0.7$ and 0.2 for $N = 100$. The longest relaxation time is computed from the relaxation function by the best fitting to the functional form[48]

$$\rho(t) = \exp(-t/\tau). \quad (4)$$

We find that the values of τ are strongly dependent on the temperature, but are roughly independent of the stripe width. We have also calculated the longest relaxation time for other polymer lengths at the typical temperatures $T = 0.7$ and 0.2. The results are shown in Fig. 2c in log–log scales for $N = 40$, 60, 80, 100 and 200. We find that the relaxation time $\tau = 2.5N^{2.13}$ MCS is sufficient for the equilibration runs. Therefore, at each temperature in the annealing process, the polymer is first equilibrated at about $\tau = 2.5N^{2.13}$ MCS,[42] and then the polymer conformation is recorded at every 0.1τ MCS in the next 100τ MCS. The results are averaged over 1000 conformations for one independent run. And the final results are averaged over 1000 independent runs.

3.2. Adsorption properties

Polymer chains will be adsorbed on the surface at low temperature or desorbed from the surface at high temperature. The adsorption or desorption state can be distinguished from the contact number n_A of the polymer in contact with the attractive stripes. For simplification, we define a desorption state as that in which there is no monomer in contact with the attractive surface, *i.e.* $n_A = 0$. In each simulation sample, we calculate the desorption probability P_d of the polymer at different temperatures by counting the number of desorption states, n_d, in the total 1000 conformations, *i.e.* $P_d = n_d/1000$. The mean desorption probability $\langle P_d \rangle$ describes how often a polymer is away from the surface.

We have calculated $\langle P_d \rangle$ for different polymer chains with lengths $N = 50$, 100, and 200 and for different stripe widths $L =$ 1, 2, 4, 8, 16, 32, and 50. The dependence of $\langle P_d \rangle$ on the temperature T for a typical chain length $N = 200$ and for different stripe widths L is shown in the inset (a) of Fig. 3. Results for other chain lengths also show similar qualitative behavior. The mean desorption probability $\langle P_d \rangle$ approaches an asymptotic value P_∞ at high temperatures, and it decreases fast to 0 at low temperatures. The temperature at which $\langle P_d \rangle$ shows the sharpest decrease is defined as the critical desorption temperature $T_{ca}(L)$. It is clear from the inset (a) of Fig. 3 that $T_{ca}(L)$ is a function of the stripe width L, which increases with the stripe width L. We find that T_{ca} can be expressed as $T_{ca}(L) = 1.60 - aL^{-1/\delta}$ with $a = 0.75$ and $\delta = 3$ as shown in the inset (b) of Fig. 3 where $[1.60 - T_{ca}(L)]$ is plotted against L in log–log scales. The results show that the critical desorption temperature for a chain length $N = 200$ is about 1.60 for an infinitely large L. The value is in agreement with the critical adsorption temperature of polymers on homogeneous surfaces for the same polymer model.[13] As the adsorption temperature increases with the chain length, we find that $T_{ca}(L \to \infty) = 1.60$ for $N = 200$ is a little smaller than 1.65 for an infinitely long chain.[13]

Furthermore, $\langle P_d \rangle$ can be roughly overlapped by rescaling T and L as $[T - T_{ca}(L \to \infty)]L^{1/\delta}$ as shown in the main panel of Fig. 3. It indicates that the adsorption/desorption behaviors of polymers on different patterned surfaces are similar. The asymptotic behavior of the desorption probability $\langle P_d \rangle$ at different temperatures T and different stripe lengths L can be expressed as

$$\langle P_d \rangle(T, L) \approx \begin{cases} P_\infty, & \text{at } [T - T_{ca}(L \to \infty)]L^{1/\delta} > -a \\ 0, & \text{at } [T - T_{ca}(L \to \infty)]L^{1/\delta} < -a \end{cases}, \quad (5)$$

where $\delta = 3$, $T_{ca} = 1.60$ and $a = 0.75$ for $N = 200$. For every curve in Fig. 3, the value $[T_{ca}(L \to \infty) - T_{ca}(L)]L^{1/\delta}$ is roughly equal to a. Therefore $T_{ca}(L)$ separates the polymer from a desorption state above $T_{ca}(L)$ to an adsorption state below $T_{ca}(L)$. Because we define a desorption state as $n_A = 0$, and the polymer can come in contact with the surface through random diffusion at a temperature far above $T_{ca}(L)$, we see that the asymptotic value P_∞ is always less than 1 in the finite system. However P_∞ increases with increase in the system size D in the surface normal direction.

The adsorption energy $E = -\varepsilon_A n_A$ is an important quantity to describe the adsorption of a polymer. The energy is proportional to the surface contact number n_A, thus n_A can be adopted as an order parameter to describe the degree of adsorption. In our simulation, we have calculated n_A for chain lengths $N = 50$, 100, and 200 and for different stripe widths L. The dependence of the mean surface contact number $\langle n_A \rangle$ of the polymer with $N = 200$ on temperature T is shown in Fig. 4a. Results of other chain lengths also exhibit similar qualitative behavior. The value of $\langle n_A \rangle$ is roughly 0 at high temperature, then shows a monotonous increase with decrease in temperature, and finally $\langle n_A \rangle$ is close to N at low temperatures. The value of $\langle n_A \rangle$ not only depends on the temperature T, but also on the stripe width L. We find that $\langle n_A \rangle$ increases with increasing L at the intermediate temperature region.

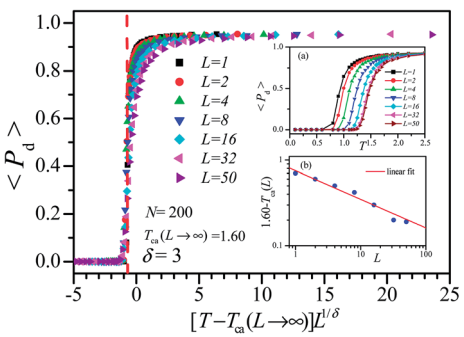

Fig. 3 Dependence of desorption probability $\langle P_d \rangle$ on the temperature T and the stripe width L for the polymer with length $N = 200$. The inset (a) presents the desorption probability at different temperatures, and the inset (b) presents the dependence of the critical desorption temperature T_{ca} on the stripe width L.

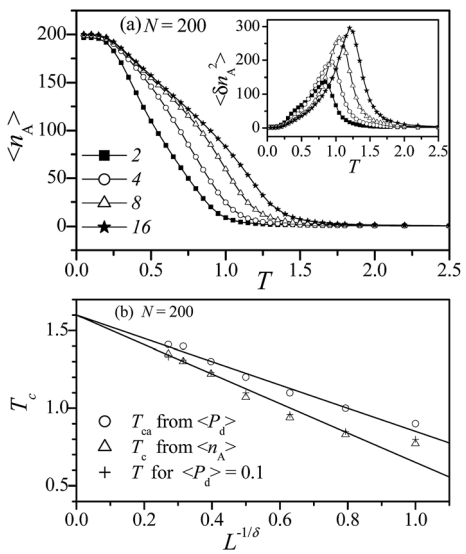

Fig. 4 (a) Dependence of the average surface contact number $\langle n_A \rangle$ and the fluctuation $\langle \delta n_A^2 \rangle$ (inset) on the temperature for a chain length $N = 200$ at different stripe widths $L = 2$, 4, 8, and 16. (b) Dependence of T_c on L for the two methodologies, from the desorption probability $\langle P_d \rangle$ and from the peak of the fluctuations of n_A, respectively. The temperature at which $\langle P_d \rangle = 0.1$ is also presented in (b).

The energy fluctuations can provide useful information for understanding the critical adsorption transition.[31] The CAP can be determined from the position of the maximum in the specific heat that is obtained by calculating the energy fluctuations which is expressed as $\langle \delta E^2 \rangle = \langle E^2 \rangle - \langle E \rangle^2$ or $\langle \delta {n_A}^2 \rangle = \langle {n_A}^2 \rangle - \langle n_A \rangle^2$. The peak of the fluctuation $\langle \delta {n_A}^2 \rangle$ indicates the place of the critical adsorption temperature $T_c(N, L)$.[18,31] The results $\langle \delta {n_A}^2 \rangle$ for $N = 200$ and for different stripe widths $L = 2$, 4, 8, and 16 are presented in the inset of Fig. 4a. It is clear that the critical adsorption temperature $T_c(L)$ increases with L for $N = 200$.

We have compared $T_c(L)$ obtained from the fluctuation $\langle \delta {n_A}^2 \rangle$ and $T_{ca}(L)$ obtained from the desorption probability $\langle P_d \rangle$. Values $T_c(L)$ and $T_{ca}(L)$ of $N = 200$ are plotted in Fig. 4b. We find that the value $T_c(L)$ is slightly lower than but close to $T_{ca}(L)$; however, the difference dies away with increase in L. $T_c(L)$ can be expressed as $T_c(L) = 1.60 - a'L^{-1/\delta}$ with $\delta = 3$ and $a' = 0.95$. It indicates that $T_c(L) = T_{ca}(L) = 1.60$ for $N = 200$ at $L \to \infty$. The value of the parameter a' is slightly bigger than that of a, as $T_c(L)$ decreases faster than $T_{ca}(L)$ with the decrease in the stripe width. As shown in Fig. 4 the temperature T_{ca} is defined as the place $\langle P_d \rangle$ that has the sharpest decrease where we find $\langle P_d \rangle \approx 0.4$. However if we define T_{ca} at which $\langle P_d \rangle = 0.1$, we find that it can well match $T_c(L)$ as shown in Fig. 4b. In the following sections of the paper, the mentioned critical adsorption temperature T_c is obtained from the fluctuation $\langle \delta {n_A}^2 \rangle$.

At the same L, the critical adsorption temperature $T_c(N, L)$ increases with the chain length N. The dependence of $T_c(N, L)$ on N is presented in Fig. 5a for different stripe widths. A linear dependence of $T_c(N, L)$ on $N^{-\phi}$ is found for all stripe widths L, where ϕ is the crossover exponent. We find $\phi = 0.5$ for all L, indicating that ϕ is independent of L for polymer adsorption on the stripe-patterned surface. By extrapolating each curve to an infinitely long chain,[49] we have estimated $T_c(L)$ for an infinitely long chain. It is evident from Fig. 5a that $T_c(L)$ increases with L. We find that $T_c(L)$ follows approximately a scaling relationship $T_c(L) = 1.65 - bL^{-1/\delta}$ with $\delta = 3$ and $b = 0.95$ as plotted in Fig. 5b. Here the value 1.65 is the critical adsorption temperature of an infinitely long polymer on a surface with an infinitely wide stripe, which is in agreement with the critical adsorption temperature of an infinitely long polymer on a homogeneous surface.[13] The value $b = 0.95$ is same as that of $a' = 0.95$ for a finite polymer length $N = 200$ in Fig. 4b.

The surface contact number, n_A, obeys the limiting scaling behavior[10,48–52]

$$n_A \sim \begin{cases} \xi & \text{for} \quad T > T_c \\ N^{\phi} & \text{for} \quad T = T_c \\ N & \text{for} \quad T < T_c \end{cases}, \tag{6}$$

where ϕ is the cross-over exponent, and ξ, which is dependent on the scaled surface separation distance $\Delta = D/(N^{\nu}b_1)$, is close to 0 for large Δ.[13] By defining a scaled temperature, $t' = T/T_c - 1$, the mean surface contact number $\langle n_A \rangle$ can be expressed as a scaling law of the form

$$\frac{\langle n_A \rangle}{N^{\phi}} \sim f_1\left(t'N^{\phi}\right) \text{ with } f_1(x) = \begin{cases} \xi x^{-1}, & \text{for} \quad x \to \infty \\ \text{const}, & \text{for} \quad x = 0 \\ (-x)^{(1/\phi)-1}, & \text{for} \quad x \to -\infty \end{cases}. \tag{7}$$

In Fig. 6 we present the scaled surface contact number, $\langle n_A \rangle / N^{\phi}$, in terms of the parameter $t'N^{\phi}$ for $L = 3$ and $L = 5$. The simulation results are in good agreement with the predictions of eqn (7).

When the chain length N is much larger than the stripe width L, the chain may be adsorbed to two or more attractive stripes below $T_c(N, L)$. This results in a multi-stripe adsorbed state with one or more bridges. The number of bridges, n_{br}, and the number of monomers on the bridges, M_{br}, are counted during the simulation. Fig. 7 shows the variation of the mean number of monomers on bridges $\langle M_{br} \rangle$ with the temperature T for different chain lengths N and different stripe widths L. The value $\langle M_{br} \rangle$ first increases with decrease in temperature, then it decreases with decrease in temperature after reaching the

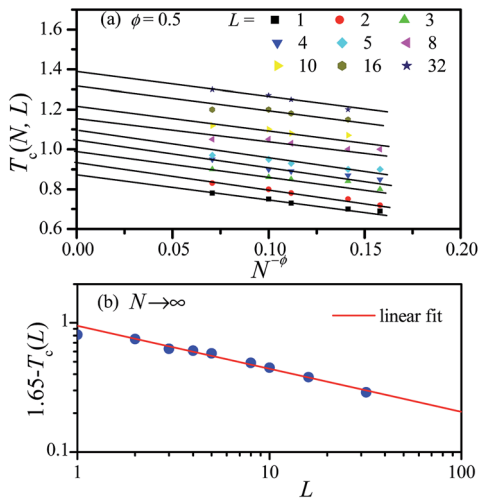

Fig. 5 (a) Dependence of the critical adsorption temperatures T_c on the chain length N for stripe widths $L = 1$, 2, 3, 4, 5, 8, 10, 16 and 32 and (b) dependence of T_c on L for an infinitely long polymer.

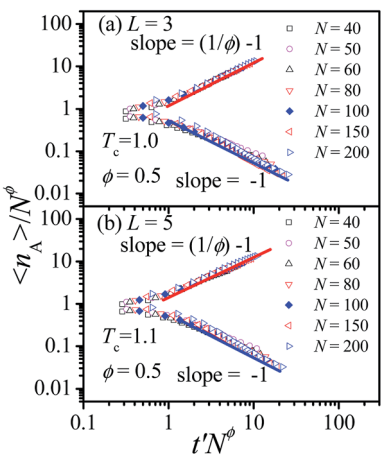

Fig. 6 Dependence of the scaled surface contact number, $\langle n_A \rangle / N^{\phi}$, on the scaling variable $t'N^{\phi}$, using the values $\phi = 0.5$, $T_c = 1.0$ for $L = 3$ (a) and $T_c = 1.1$ for $L = 5$ (a).

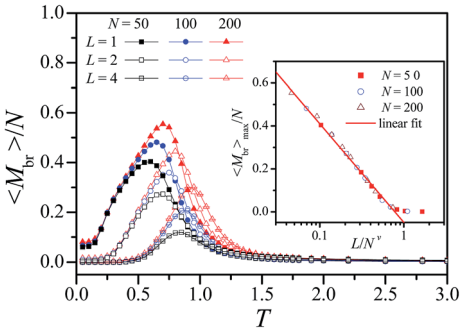

Fig. 7 Dependence of the mean fraction of monomers on bridges $\langle M_{br}\rangle/N$ on the temperature T for different stripe widths L and chain lengths N. The inset presents the dependence of the maximum $\langle M_{br}\rangle_{max}/N$ on L/N^{ν}. $\nu = 0.588$ is the Flory exponent.

maximum $\langle M_{br}\rangle_{max}$. We present the dependence of $\langle M_{br}\rangle_{max}/N$ on L/N^{ν} for $N = 50$, 100 and 200 in the inset of Fig. 7. Here $\nu \approx 0.588$ is the Flory exponent. We find that $L/N^{\nu} < 1$ is one of the necessary conditions for forming bridges for a finitely long polymer.

The mean bridge number $\langle n_{br}\rangle$ of the polymer is also calculated. The behavior of $\langle n_{br}\rangle$ is similar to $\langle M_{br}\rangle$. The dependence of $\langle n_{br}\rangle$ on the temperature is presented in Fig. 8 for different stripe widths L. We find that bridges occur below $T_c(N, L)$. The bridge number first increases with decrease in the temperature, then it decreases with decrease in the temperature after $\langle n_{br}\rangle$ reaches the maximum. Therefore there is a transition temperature at which the polymer is in contact with multiple attractive stripes to one single attractive stripe. So we refer to it as the critical pattern-recognition temperature T_r as defined in the literature.[19] Below T_r, both $\langle n_{br}\rangle$ and $\langle M_{br}\rangle$ tend to 0. The value of T_r is estimated by extrapolating the straight line with the maximum slope of the $\langle n_{br}\rangle$–T curve to 0. We find that T_r is slightly dependent on the chain length N but is strongly dependent on the stripe width L.

It is evident from Fig. 7 and 8 that bridges start at T_c but disappear at T_r for all L except $L = 1$, *i.e.* the bridges only exist at the intermediate temperature $T_r < T < T_c$. The critical pattern-recognition temperature $T_r(N, L)$ has been estimated for different polymer lengths and different stripe widths. We find that the results for $T_r(N, L)$ can be scaled as a function of N^{-1}, and we can obtain the value of the critical pattern-recognition temperature $T_r(L) = \lim_{N\to\infty} T_r(N, L)$ for an infinitely long chain by extrapolating $N^{-1} \to 0$. The results of $T_r(L)$ are presented in the inset of Fig. 8. An approximation relationship is observed as $T_r(L) = 1.65 - cL^{-1/\delta}$ with $\delta = 3$ and $c = 1.7$. It is clearly seen that, in the case of an infinitely wide stripe, a phase transition occurs at about $T_r = 1.65$ for an infinitely long polymer. The value δ is the same as that for the critical adsorption $T_c(L)$ shown in Fig. 5. It is interesting to see that both $T_c(L)$ and $T_r(L)$ follow the same scaling relationship with the same exponent, indicating that the physics governing the two transitions is similar.

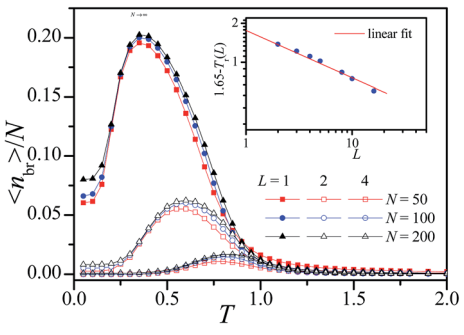

Fig. 8 Dependence of the fraction of the bridge number $\langle n_{br}\rangle/N$ on the temperature for chain length $N = 50$, 100, and 200 on different stripe widths $L = 1$, 2, and 4. The inset presents the dependence of the critical pattern-recognition temperature T_r on the stripe width for an infinitely long chain.

Our results show that the polymer is adsorbed on the stripe-patterned surface at $T_c(L)$ and on the single attractive stripe at $T_r(L)$. From the expression of the free energy $F = U - TS$, the two transitions can be explained from the competition between the energy U and the entropy S of the polymer. When the decrease in U exceeds the decrease in S due to the adsorption, the critical adsorption occurs at $T_c(L)$. It is obvious that adsorption on the single attractive stripe will decrease both U and S. Similarly, with further decrease in the temperature, the decrease in U exceeds the decrease in S again, the critical pattern-recognition occurs at $T_r(L)$. Therefore, the physics for the two transitions may be analogous.

3.3. Phase diagram

Using the critical adsorption temperature $T_c(L)$ and the critical pattern-recognition temperature $T_r(L)$, one can construct a phase diagram for an infinitely long polymer. This is one of the key results of the present study. Fig. 9 presents the phase diagram for an infinitely long polymer on the stripe-patterned surface, which shows the three states of the polymer in the T–L^{-1} plane. At a high temperature $T > T_c(L)$, the polymer is desorbed from the surface for all the values of the stripe width L considered in this work. At the intermediate temperature $T_r(L) < T < T_c(L)$, the polymer is adsorbed on the surface and comes into contact with multiple A-stripes for a finite stripe width L. At a low temperature $T < T_r(L)$, the polymer is adsorbed on a single A-stripe for all the values of the stripe width L except $L = 1$. Evidently, the critical adsorption temperature and the critical pattern-recognition temperature for an infinitely wide stripe appear to be in good agreement with the critical adsorption temperature for homogeneous surfaces.[13] We identify transition lines in the space of field variables T and L that separate the three regions of the polymer in the desorbed state (DS), in the multi-stripe adsorbed state (MSAS), and in the single-stripe adsorbed state (SSAS).

For a finite chain length and finite stripe width, we perform the simulation to calculate the probability of samples in DS ($n_A = 0$), MSAS ($n_A > 0$, $n_{br} > 0$) and SSAS ($n_A > 0$, $n_{br} = 0$) at the different temperatures T, which are marked as P_{DS}, P_{MSAS} and P_{SSAS}, respectively. After equilibrium, we record 1000 polymer conformations at every time interval 0.1τ MCS in each simulation sample. Thus we obtain values P_{DS}, P_{MSAS} and P_{SSAS} in one

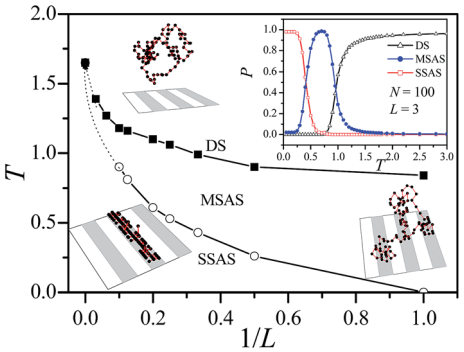

Fig. 9 Phase diagram of the polymer on a stripe-patterned surface composed of periodical attractive and neutral stripes in the limit $N \to \infty$. The phases are separated into three regions on the T–L^{-1} plane: DS for $T > T_c$, MSAS for $T_r < T < T_c$, and SSAS for $T < T_r$, respectively. The inset presents the probability of samples with $n_A = 0$ (DS), $n_A > 0$ and $n_{br} > 0$ (MSAS), and $n_A > 0$ and $n_{br} = 0$ (SSAS) as a function of the temperature T for chain length $N = 100$, stripe length $L = 3$ and the surface space distance $D = 100$.

simulation sample by counting the number of the three states. They are then averaged over 1000 independent simulation samples. The dependence of P_{DS}, P_{MSAS} or P_{SSAS} on the temperature T is presented in the inset of Fig. 9 for $N = 100$, $L = 3$ and $D = 100$. At high temperature $T > T_c$, the polymer is desorbed from the stripe-patterned surface, so we find $P_{DS} = 1$, $P_{MSAS} = 0$ and $P_{SSAS} = 0$, respectively. Near T_c, the value of P_{DS} decreases sharply but the value of P_{MSAS} increases with the decrease in temperature T. Below T_c, the surface contact number increases with decrease in T. Therefore, at the intermediate temperature $T_r < T < T_c$, the value of P_{MSAS} first increases with decrease in T and then decreases after reaching the maximum $P_{MSAS} = 1$. Near T_r, the value of P_{MSAS} decreases but the value of P_{SSAS} increases with decrease in T. At the low temperature $T < T_r$, the polymer is adsorbed on a single stripe. Hence, the probability of samples in DS, MSAS and SSAS is $P_{DS} = 0$, $P_{MSAS} = 0$ and $P_{SSAS} = 1$, respectively.

3.4. Conformational properties

We have studied the conformational properties of the polymer in different phases as shown in Fig. 9. We thus calculated the mean square radius of gyration $\langle R_G^2 \rangle$ and the mean asphericity parameter $\langle A \rangle$ for the polymer in DS, MSAS, SSAS, respectively. The asphericity parameter A can be defined as

$$A = \sum_{i>j}^{3} \left(L_i^2 - L_j^2\right)^2 \Big/ 2\left(\sum_{i=1}^{3} L_i^2\right)^2 \quad (8)$$

in three-dimensional space.[45] Here, L_1^2, L_2^2, and L_3^2 ($L_1^2 \le L_2^2 \le L_3^2$) are the three eigenvalues of the radius of gyration tensor S. The radius of gyration tensor S can be defined as

$$S = \frac{1}{n}\sum_{i=1}^{n} s_i s_i^T = \begin{pmatrix} S_{xx} & S_{xy} & S_{xz} \\ S_{xy} & S_{yy} & S_{yz} \\ S_{xz} & S_{yz} & S_{zz} \end{pmatrix}. \quad (9)$$

where $s_i = \mathrm{col}(x_i, y_i, z_i)$ represents the position of the ith monomer in the frame of the reference with its origin at the center of mass.[45] s_i^T is the transposed matrix of s_i. The mean asphericity parameter $\langle A \rangle$ is calculated at different temperatures. The dependence of $\langle A \rangle$ on the temperature T is plotted in Fig. 10a for $N = 200$ and $L = 5$. The value of $\langle A \rangle$ is about 0.40, which indicates that the polymer is in a 3D random coil configuration, at high temperature $T > T_c$. The value $\langle A \rangle$ increases to 1 at low temperature $T < T_r$, indicating that the polymer is in a 1D configuration. The value of $\langle A \rangle$ changes from about 0.40 to 1.0 at the temperature from T_c to T_r, which indicates that the configuration of the polymer changes from 3D to 1D. The transition temperature span of the polymer from 3D to 1D is in agreement with the temperature regions $T_r < T < T_c$.

The mean square radius of gyration $\langle R_G^2 \rangle$ is also plotted in Fig. 10a. Analogous to $\langle A \rangle$, the increase of $\langle R_G^2 \rangle$ starts at T_c. However, we find $\langle R_G^2 \rangle$ increases continuously even below T_r. We find that the scaling $\langle R_G^2 \rangle \sim N^{2\nu}$ exists at all temperatures as shown in the inset of Fig. 10b. The exponent ν is plotted *versus* the temperature for $L = 5$ in Fig. 10b. At a high temperature $T > T_c$, $\nu \approx 0.6$ indicates that the polymer is in a 3D configuration, whereas at a low temperature $T < T_r$, $\nu \approx 1$ indicates that the polymer is in a 1D one. The results are consistent with the theoretical prediction $\nu = 3/(d + 2)$ where d is the dimension of space.[53] Both $\langle A \rangle$ and ν indicate that the configuration of the polymer changes from the 3D behavior above T_c to the 1D behavior below T_r.

3.5. Diffusion properties

Finally, the diffusion characteristics of the polymer are studied. The mean-square displacement of the center-of-mass of a single polymer chain

$$\langle \Delta r^2 \rangle = \langle [r_{cm}(t) - r_{cm}(0)]^2 \rangle \quad (10)$$

is calculated at different times. Here $r_{cm}(t)$ and $r_{cm}(0)$ are the position vectors of the center-of-mass at time t and at starting

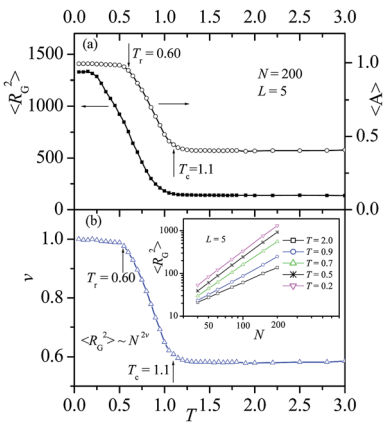

Fig. 10 (a) Dependence of the mean square radius of gyration $\langle R_G^2 \rangle$ and the mean asphericity parameter $\langle A \rangle$ on temperature T for $L = 5$ and $N = 200$, (b) dependence of the exponent ν in $\langle R_G^2 \rangle \sim N^{2\nu}$ on temperature T for $L = 5$, and the dependence of $\langle R_G^2 \rangle$ on N for $T = 2$, 0.9, 0.7, 0.5 and 0.2 in the inset of (b).

time $t = 0$, respectively. As the polymer is adsorbed on the surface below T_c, we only calculate the components parallel to the surface, *i.e.* perpendicular to the stripe $\langle \Delta r^2 \rangle_x$ and parallel to the stripe $\langle \Delta r^2 \rangle_y$, respectively. Fig. 11 presents the evolution of $\langle \Delta r^2 \rangle_x$ and $\langle \Delta r^2 \rangle_y$ for a chain length $N = 100$ and stripe width $L = 5$ at different temperatures $T = 2$, 0.7 and 0.2, respectively. Here, both $\langle \Delta r^2 \rangle_x$ and $\langle \Delta r^2 \rangle_y$ show the same behavior at high temperature $T = 2 (T > T_c)$. But they show different behaviors at the intermediate temperature $T = 0.7 (T_r < T < T_c)$ and at low temperature $T = 0.2 (T < T_r)$.

At high temperature $T = 2$ (Fig. 11a), normal diffusions $\langle \Delta r^2 \rangle_x \propto t$ and $\langle \Delta r^2 \rangle_y \propto t$ are observed and $\langle \Delta r^2 \rangle_x$ is roughly equal to $\langle \Delta r^2 \rangle_y$. The results indicate that the polymer diffuses roughly freely at high temperature $T > T_c$ (in DS). In this case, the heterogeneous surface does not introduce anisotropy for the polymer diffusion. At intermediate temperature $T = 0.7$ (in MSAS), the polymer is adsorbed on the stripe-patterned surface. As shown in Fig. 11b, in the direction perpendicular to the stripe, abnormal diffusion appears at a short time scale, but the polymer diffuses normally at a long time scale. Whereas normal diffusion $\langle \Delta r^2 \rangle_y \propto t$ is always observed in the direction parallel to the stripe. However, at a long time scale, the diffusion constant in the x direction is smaller than that in the y direction. These results indicate that polymer diffusion is affected by the heterogeneous surface at the intermediate temperature $T_r < T < T_c$ (in MSAS). At low temperature $T = 0.2$ (Fig. 11c, $T < T_r$, SSAS), although the polymer diffuses normally along the parallel direction at a long time scale, $\langle \Delta r^2 \rangle_x$ does not increase with time. The polymer adsorbed on one single stripe is restricted to diffusion inside the attractive stripe. Since the system is uniform along the parallel direction, we find that normal diffusion along the parallel direction will always exist at any temperature. But diffusion in the direction perpendicular to the stripe is significantly influenced by the anisotropy of the surface.

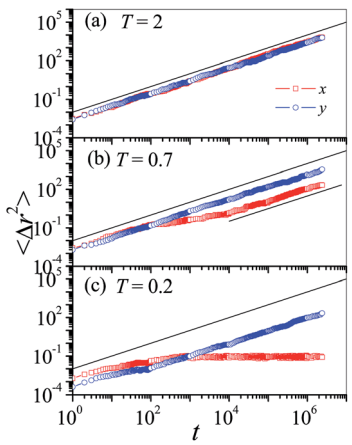

Fig. 11 The mean square displacement of the polymer parallel to the surface, $\langle \Delta r^2 \rangle_x$ in the direction perpendicular to the stripe and $\langle \Delta r^2 \rangle_y$ in the direction parallel to the stripe for $N = 100$ and $L = 5$ at (a) $T = 2$, (b) $T = 0.7$ and (c) $T = 0.2$, respectively. Solid lines have a slope equal to 1, indicating a normal diffusion of the polymer. The unit of time t is MCS.

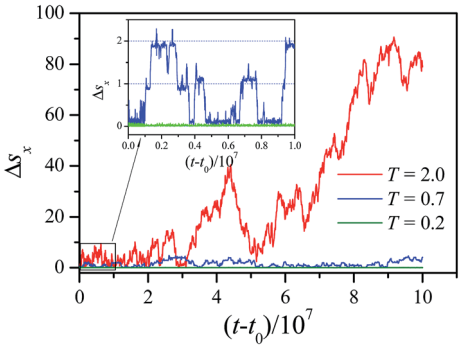

Fig. 12 The scaled displacement of the polymer parallel to the surface in the x direction, Δs_x, for chain length $N = 100$ and stripe width $L = 5$ at temperatures $T = 0.2$, 0.7, and 2 in a long time scale. The inset presents Δs_x at $T = 0.2$, and 0.7 in a short time scale. The unit of time t is MCS.

To further understand the diffusion behavior of the polymer in the direction perpendicular to the stripe, we introduce a rescaled displacement

$$\Delta s_x = \frac{\sqrt{\langle \Delta r^2 \rangle_x}}{2L}. \quad (11)$$

It is clear that Δs_x measures the diffusion of the polymer in the unit of a pattern period $2L$. Fig. 12 shows the evolution of the rescaled displacement Δs_x for chain length $N = 100$ and stripe width $L = 5$ at temperatures $T = 0.2$, 0.7, and 2 for one typical simulation run. Above the critical adsorption temperature $T > T_c$ (*e.g.* $T = 2$ in DS), Δs_x changes continuously with t, indicating that the polymer diffuses freely in the x direction. At intermediate temperature $T_r < T < T_c$ (*e.g.* $T = 0.7$ in MSAS), Δs_x remains at integer values for a relatively long time period but shifts its value quickly. The long period constant of Δs_x means that the polymer is trapped in the x direction while the integer value of Δs_x means that the polymer moves forward or backward one period globally. The change of Δs_x shows that, in the direction perpendicular to the stripe, adsorption and desorption take place frequently. However, the polymer stays in the adsorbed state for a relatively long time period that reduces the diffusion of the polymer at $T = 0.7$. The results show that the polymer adsorbed simultaneously on multiple attractive stripes may hop to the neighboring attractive stripe. At even low temperature $T < T_r$ (*e.g.* $T = 0.2$ in SSAS) Δs_x is close to 0, indicating that the polymer is trapped inside one stripe and cannot hop between two neighboring stripes. In this case, the polymer can diffuse along the parallel direction but the neighboring stripe hop is forbidden.

4. Conclusions

In this paper, the adsorption and dynamics of polymers on a stripe-patterned surface with alternating attractive and neutral stripes are studied using Monte Carlo simulations. The critical adsorption temperature T_c and pattern-recognition temperature T_r are estimated from the desorption probability, surface contact number, and bridge number. We find that both T_c and

T_r increase with increase in the stripe width L and have similar scaling relationships $T_c(L) = 1.65 - bL^{-1/\delta}$ and $T_r(L) = 1.65 - cL^{-1/\delta}$ with $\delta = 3$, $b = 0.95$ and $c = 1.7$ for an infinitely long polymer, respectively. We found that there are three phases for infinitely long polymers on the stripe-patterned surface including the desorbed state above T_c, multi-stripe adsorbed state between T_c and T_r, and single-stripe adsorbed state below T_r. Corresponding to these three temperature regions, configurations of the polymer are in 3D above T_c, from 3D to 1D between T_c and T_r, and in 1D below T_r for an infinitely long polymer on the stripe-patterned surface with the finite width L. The temperature span of the polymer adsorbed on multi-stripes decreases with increase in L. However, for finitely long polymers the existence of the multi-stripe adsorbed state is restricted to narrow stripes with $L/N^{\nu} < 1$. We found that the dependence of the mean asphericity parameter $\langle A \rangle$ or the exponent ν on T is similar near T_c and T_r, where they are constant above T_c or below T_r. The dynamics of an adsorbed polymer is described by the self-diffusion of the polymer. In the direction perpendicular to the stripe, normal diffusion is observed at high temperature $T > T_c$, but the polymer is limited to one attractive stripe at low temperature $T < T_r$. In the intermediate temperature $T_r < T < T_c$, the diffusion is slowed down but the polymer can hop between different stripes, therefore a normal diffusion is observed at long time scales. However, our results show that the polymer can always diffuse along the stripe at any temperature.

Acknowledgements

This work was supported by the National Natural Science Foundation of China under Grant nos 11304231, 11374255, 11474222 and 21171145.

References

1 J. M. Goddard and J. H. Hotchkiss, *Prog. Polym. Sci.*, 2007, **32**, 698–725.
2 A. Milchev and K. Binder, *Macromolecules*, 1996, **29**, 343–354.
3 J. Paturej, A. Milchev, V. G. Rostiashvili and T. A. Vilgis, *Macromolecules*, 2012, **45**, 4371–4380.
4 K. Kato, E. Uchida, E.-T. Kang, Y. Uyama and Y. Ikada, *Prog. Polym. Sci.*, 2003, **28**, 209–259.
5 H. Zeng, *Polymer Adhesion, Friction, and Lubrication*, John Wiley & Sons, 2013.
6 A. Ginzburg, T. Macko, V. Dolle and R. Brüll, *Eur. Polym. J.*, 2011, **47**, 319–329.
7 M. Motornov, Y. Roiter, I. Tokarev and S. Minko, *Prog. Polym. Sci.*, 2010, **35**, 174–211.
8 J. Topinka, J. Hovorka, A. Milcova, J. Schmuczerova, J. Krouzek, P. Rossner Jr and R. J. Sram, *Toxicol. Lett.*, 2010, **198**, 304–311.
9 N. N. Oskolkov, P. Linse, I. I. Potemkin and A. R. Khokhlov, *J. Phys. Chem. B*, 2011, **115**, 422–432.
10 E. Eisenriegler, K. Kremer and K. Binder, *J. Chem. Phys.*, 1982, **77**, 6296–6320.
11 R. Descas, J.-U. Sommer and A. Blumen, *Macromol. Theory Simul.*, 2008, **17**, 429–453.
12 M. B. Luo, *J. Chem. Phys.*, 2008, **128**, 044912.
13 H. Li, C. J. Qian, C. Wang and M. B. Luo, *Phys. Rev. E: Stat., Nonlinear, Soft Matter Phys.*, 2013, **87**, 012602.
14 J. Luettmer-Strathmann, F. Rampf, W. Paul and K. Binder, *J. Chem. Phys.*, 2008, **128**, 064903.
15 H. Li, C. J. Qian, L. Z. Sun and M. B. Luo, *Polym. J.*, 2010, **42**, 383–385.
16 H. Li, C. J. Qian and M. B. Luo, *J. Appl. Polym. Sci.*, 2012, **124**, 282–287.
17 A. Sikorski, *Macromol. Theory Simul.*, 2002, **11**, 359–364.
18 P. A. Sánchez, J. J. Cerdà, V. Ballenegger, T. Sintes, O. Piro and C. Holm, *Soft Matter*, 2011, **7**, 1809–1818.
19 J. J. Cerda and T. Sintes, *Biophys. Chem.*, 2005, **115**, 277–283.
20 F. A. Denis, A. Pallandre, B. Nysten, A. M. Jonas and C. C. Dupont-Gillain, *Small*, 2005, **1**, 984–991.
21 Y. Wang, Z. Liu, Y. Huang, B. Han and G. Yang, *Langmuir*, 2006, **22**, 1928–1931.
22 E. Glynos, A. Chremos, G. Petekidis, P. J. Camp and V. Koutsos, *Macromolecules*, 2007, **40**, 6947–6958.
23 X. C. Chen, H. M. Li, F. Fang, Y. W. Wu, M. Wang, G. B. Ma, Y. Q. Ma, D. J. Shu and R. W. Peng, *Adv. Mater.*, 2012, **24**, 2637–2641.
24 K. Kargupta and A. Sharma, *J. Chem. Phys.*, 2002, **116**, 3042–3051.
25 K. G. A. Tavakkoli, K. W. Gotrik, A. F. Hannon, A. Alexander-Katz, C. A. Ross and K. K. Berggren, *Science*, 2012, **336**, 1294–1298.
26 J. Xu, T. P. Russell, B. M. Ocko and A. Checco, *Soft Matter*, 2011, **7**, 3915–3919.
27 P. Andrew and W. T. S. Huck, *Soft Matter*, 2007, **3**, 230–237.
28 H. Chen, X. Chen, Z. Ye, H. Liu and Y. Hu, *Langmuir*, 2010, **26**, 6663–6668.
29 A. Al Sunaidi, *Macromol. Theory Simul.*, 2007, **16**, 86–92.
30 A. Al Sunaidi, *Macromol. Theory Simul.*, 2008, **17**, 319–324.
31 K. Sumithra, *J. Chem. Phys.*, 2009, **130**, 194903.
32 B. Patel, J. D. Ziebarth and Y. M. Wang, *Macromolecules*, 2010, **43**, 2069–2075.
33 H. Tran, K. L. Killops and L. M. Campos, *Soft Matter*, 2013, **9**, 6578–6586.
34 K. Sumithra and E. Straube, *J. Chem. Phys.*, 2006, **125**, 154701.
35 K. Sumithra and E. Straube, *J. Chem. Phys.*, 2007, **127**, 114908.
36 K. Sumithra, M. Brandau and E. Straube, *J. Chem. Phys.*, 2009, **130**, 234901.
37 P. Adamczyk, P. Romiszowski and A. Sikorski, *Catal. Lett.*, 2008, **129**, 130–134.
38 S. Jaworski and A. Sikorski, *Polymer*, 2012, **53**, 1741–1746.
39 J. McNamara, C. Y. Kong and M. Muthukumar, *J. Chem. Phys.*, 2002, **117**, 5354–5360.
40 H. Li, C. J. Qian and M. B. Luo, *Polym. Polym. Compos.*, 2012, **20**, 107–110.
41 L. Carlacci and S. W. Englander, *Biopolymers*, 1993, **33**, 1271–1286.
42 M. B. Luo and J. H. Huang, *J. Chem. Phys.*, 2003, **119**, 2439–2443.

43 S. M. Hur, A. L. Frischknecht, D. L. Huber and G. H. Fredrickson, *Soft Matter*, 2011, **7**, 8776–8788.
44 J. H. Huang, Z. X. Fan and Z. X. Ma, *J. Chem. Phys.*, 2013, **139**, 064905.
45 H. Li, C. J. Qian, J. H. Huang and M. B. Luo, *Polym. J.*, 2015, **47**, 53–58.
46 D. Hofmann, L. Fritz, J. Ulbrich, C. Schepers and M. Böhning, *Macromol. Theory Simul.*, 2000, **9**, 293–327.
47 N. C. Karayiannis, V. G. Mavrantzas and D. N. Theodorou, *Macromolecules*, 2004, **37**, 2978–2995.
48 A. L. Ponomarev, T. D. Sewell and C. J. During, *Macromolecules*, 2000, **33**, 2662–2669.
49 K. Sumithra and A. Baumgaertner, *J. Chem. Phys.*, 1999, **110**, 2727–2731.
50 S. Bhattacharya, H. P. Hsu, A. Milchev, V. G. Rostiashvili and T. A. Vilgis, *Macromolecules*, 2008, **41**, 2920–2930.
51 S. Metzger, M. Müller, K. Binder and J. Baschnagel, *Macromol. Theory Simul.*, 2002, **11**, 985–995.
52 M. Müller, Polymers at Interfaces and Surfaces and in Confined Geometries, in *Polymer Science: A Comprehensive Reference*, Elsevier, 2012, vol. 1, pp. 387–416.
53 M. V. Jarić and G. F. Tuthill, *Phys. Rev. Lett.*, 1985, **55**, 2891–2894.